Hydrol. Earth Syst. Sci. Discuss., doi:10.5194/hess-2016-408, 2016
Manuscript under review for journal Hydrol. Earth Syst. Sci.
Published: 24 August 2016

Hydrology and Earth System Sciences
Open Access
Discussions

Analyzing the impact of groundwater flow and storage changes on Budyko relationships across the continental US

Laura E. Condon[1*] and Reed M. Maxwell[2]

[1]Department of Civil and Environmental Engineering, Syracuse University, Syracuse, NY USA

[2]Integrated GroundWater Modeling Center, Department of Geology and Geological Engineering, Colorado School of Mines, Golden CO USA

Correspondence to: lecondon@syr.edu

Abstract:

We use a transient, integrated groundwater surface water simulation of the majority of the continental US to evaluate the impacts of groundwater surface water exchanges on Budyko relationships for roughly 25,000 nested watersheds ranging in sized from 100 km^2 to over 3,000,000 km^2. The simulation spans a single water year with varying degrees of storage change and trans-watershed lateral flow throughout the domain. This provides a test bed for evaluating the role of realistic groundwater storage changes across a range of climates and physical settings within a rigorous computational framework in which every watershed's water balance component can be fully defined. Budyko curves are compared using (1) the standard simplification where evapotranspiration is calculated as the difference between precipitation and outflow, (2) the case in which evapotranspiration is directly measured (or simulated) and (3) a modified approach where groundwater contributions are accounted for with the incoming precipitation. Results show that for all three cases, large watersheds still converge around the Budyko curve despite the fact that the equilibrium assumption is violated. However, the best results are found when groundwater interactions are directly accounted for. While the two standard approaches for inferring or directly measuring evapotranspiration still generate Budyko type behavior, the parameters of the curves vary systematically with groundwater contributions and the relationship between curve parameters and groundwater surface water exchanges is fundamentally

Hydrol. Earth Syst. Sci. Discuss., doi:10.5194/hess-2016-408, 2016
Manuscript under review for journal Hydrol. Earth Syst. Sci.
Published: 24 August 2016

Hydrology and Earth System Sciences
Open Access
Discussions

different between approaches. This results in contradictory spatial patterns depending on the calculation method and highlights the importance of evaluating uncertainty in the equilibrium assumption for any Budyko analysis, especially those that seek to attribute variability in curve parameters to physical characteristics. Finally, the shape parameter is evaluated as a function of scale and large, continental scale basins are shown to converge onto a single Budyko relationship.

1. Introduction:

The Budyko hypothesis states that the fraction of precipitation (P) that leaves a watershed through evapotranspiration (E), as opposed to runoff, can be well predicted by the aridity of the watershed [*Budyko*, 1958; 1974]. *Budyko* [1974] compared long-term evapotranspiration fractions to aridity for 1,200 large watersheds around the globe and showed that 90% of the variance in evapotranspiration ratio (E/P) could be described by a single empirical curvilinear equation dependent only on aridity, often referred to as the “Budyko Curve”. Budyko noted that this consistent relationship is a reflection of the dominance of macroclimate over large drainage areas and long time periods where it can be assumed that a watershed is in steady state.

The simplicity of this relationship has since garnered much interest within the hydrologic community for its potential to predict watershed behavior using only climate variables, which are often easier to observe than many hydrologic variables, and without relying on computationally expensive or heavily parameterized numerical models. In recent years the Budyko hypothesis has also been put forward as a way of predicting hydrologic sensitivity to climate change especially in ungauged basins [e.g. *Randall J. Donohue et al.*, 2011; *Jones et al.*, 2012; *Renner et al.*, 2014]. However, application of this method has been partially limited by spatial variability between watersheds and the required steady state assumption.

The original Budyko curve presented a universal relationship between evapotranspiration and aridity [*Budyko*, 1974]. Subsequent work has shown that, while the Budkyo curve is generally robust, the shape of the curve can vary between locations and climate alone is not sufficient to predict watershed partitioning, especially for smaller watersheds. Differences in behavior between river basins have been attributed to seasonal lags in water and energy supply, vegetative and soil properties [*R. J. Donohue et al.*, 2007]. The original Budyko curve has been reformulated multiple times to incorporate additional free parameters [*Choudhury*, 1999; *Fu*, 1981; *Milly*, 1994; *L. Zhang et al.*, 2001; *L. Zhang et al.*, 2004], and numerous studies have used these modified formulations to relate curve parameters to physical basin characteristics in many settings [e.g. *Li et al.*, 2013; *Shao et al.*, 2012; *Williams et al.*, 2012; *Xu et al.*, 2013; *Yang et al.*, 2009]. For example, *Li et al.* [2013] and *Yang et al.* [2009] evaluated relationships between the shape of the Budyko curve and vegetation coverage. Similarly, *Williams et al.* [2012] and *L. Zhang et al.* [2004] found distinct shape parameters when comparing forested watersheds to grasslands, although it should be noted that they reached the opposite conclusion about their relative magnitudes. Others have focused on the role of soil moisture and noted differences in behavior based on plant water availability and seasonal lags in supply and demand [e.g. *Milly*, 1994; *Yang et al.*, 2007; *Yokoo et al.*, 2008].

Many previous studies have demonstrated good predictive abilities using modified Budyko formulations even when applied to smaller watersheds and shorter time scales than those originally intended. However, poor performance in some locations, especially over annual or seasonal time periods, has been attributed to the influence of storage changes that violate the steady state assumption [*Milly and Dunne*, 2002; *Lu Zhang et al.*, 2008]. *Istanbulluoglu et al.* [2012] and *T Wang et al.* [2009] showed interannual storage changes can produce a negative correlation between evapotranspiration ratio and aridity that is counter to the Budyko curve for baseflow dominated basins in the Nebraska Sand Hills. *D Wang* [2012] evaluated inter-annual storage changes for twelve watersheds in Illinois and showed that, on an annual timescale, variability in runoff and storage is larger than evapotranspiration, and accounting for storage can improve the performance of Budyko predictions. *Du et al.* [2016] presented a method for explicitly accounting for storage changes within the

Budyko framework and demonstrated that this approach can greatly improve performance in arid regions or over shorter time scales where the steady state assumption is not valid. These studies all indicate the potential importance of groundwater surface water interactions within the Budyko framework, however they are based on a limited number of catchments. Further research is needed to evaluate the impact of storage changes across spatial scales and physical settings and to provide a more general understanding of this behavior.

Here we evaluate the role of groundwater surface water exchanges in the Budyko framework using an physically based hydrologic model to directly simulate the integrated groundwater surface water system over a large spatial domain at high resolution. This approach provides detailed quantitative information about subsurface fluxes, which has been a limiting factor for previous research on this topic. For example, in some previous studies, the impact of groundwater storage changes have been inferred from variability around the Budyko relationship, but the storage changes themselves were not measured [*Milly and Dunne*, 2002; *Lu Zhang et al.*, 2008]. Others have addressed interactions more directly using baseflow separation techniques that require only streamflow observations [*T Wang et al.*, 2009] or lumped watershed models that parameterize baseflow and recharge [*Du et al.*, 2016]. However, with both of these approaches the groundwater system is still not directly simulated or observed. *Istanbulluoglu et al.* [2012] and *D Wang* [2012] did use observations of water table depth to directly quantify storage changes and demonstrate the impact of this change within the Budyko framework; but the study areas with this approach were relatively limited (four watersheds for *Istanbulluoglu et al.* [2012], and twelve for *D Wang* [2012]). Groundwater observations sufficient to precisely characterize watershed storage changes are not widely available. Therefore, for this analysis we rely on simulated watersheds to evaluate the role of storage changes across a broad range of spatial scales and physiographic settings with different Budyko approaches.

Hydrol. Earth Syst. Sci. Discuss., doi:10.5194/hess-2016-408, 2016
Manuscript under review for journal Hydrol. Earth Syst. Sci.
Published: 24 August 2016

2. Methods

2.1 The use of hydrologic modeling for Budyko Analysis

Previous work has evaluated the Budyko curve using hydrologic models of varying levels of complexity. The abcd model employed by *Du et al.* [2016], among others, is a lumped water balance model that includes baseflow and groundwater recharge using calibrated parameters. *Yokoo et al.* [2008] used a different water balance model with a more complex groundwater formulation that includes saturated and unsaturated zones, but the authors noted limitations in simulating infiltration excess overland flow with this approach. *Gentine et al.* [2012] applied a water balance model that includes a soil bucket and can simulate infiltration excess overland flow; however it did not include topography and was only applied at the plot scale. While these approaches do account for storage in the subsurface and varying levels of complexity in groundwater surface water exchanges, they all take a lumped approach and rely on calibrated parameters that are not physically based.

Increasing in sophistication, *Troch et al.* [2013] used a semi-distributed model that included shallow perched aquifers as well as root zone and soil moisture dynamics; and *Koster and Suarez* [1999] evaluated a global circulation model that simulated land surface and atmospheric processes using physically based equations. The trade-off for increasing model sophistication is computational expense especially for large high-resolution domains. *Koster and Suarez* [1999] used a global simulation but at low spatial resolution (4° by 5°), while *Troch et al.* [2013] limited their analysis to the hillslope scale. Furthermore, both of these approaches are focused on the land surface and shallow subsurface and neither included lateral groundwater flow.

To the authors' knowledge, no one has evaluated Budyko behavior over large spatial scales using a hydrologic model that integrates lateral groundwater flow with surface processes. So called, integrated hydrologic models that incorporate physically based lateral groundwater flow with overland flow and land surface processes are a relatively new development in hydrologic modeling. These tools are ideal for capturing dynamic behavior and interactions throughout the terrestrial hydrologic cycle and they have been increasingly applied over the last decade. To achieve this level of complexity requires significant computational resources, and detailed model inputs. These requirements have generally limited the application of integrated tools to regional scale domains. Continental-scale high-resolution simulations have only recently become technically feasible.

2.2 Integrated Hydrologic Model

For this analysis, we use the first high-resolution integrated groundwater surface water simulation of the majority of the continental US (CONUS) [*Maxwell and Condon*, 2016; *Maxwell et al.*, 2015]. The CONUS simulation was developed using the integrated hydrologic model ParFlow-CLM [*Kollet and Maxwell*, 2006; 2008; *Maxwell and Miller*, 2005]. ParFlow simulates three-dimensional variably saturated groundwater flow using Richards' equation:

$$S_s S(\psi_p)\frac{\delta\psi_p}{\delta t} + \phi\frac{\delta S(\psi_p)}{\delta t} = \nabla\cdot\left[-K_s(x)k_r(\psi_p)\cdot\nabla(\psi_p - z)\right] + q_s \qquad (1)$$

where S_s is the specific storage [L^{-1}], S is the relative permeability [-], which varies with pressure head ψ_p [L] based on the *Van Genuchten* [1980] relationships, t is time [T], ϕ is the porosity of the subsurface [-], K_s(x) is the saturated hydraulic conductivity tensor [LT^{-1}], K_r is the relative permeability [-], which also varies with pressure head according to the *Van Genuchten* [1980] relationships, z is the depth below the surface [L] and q_s is a source/sink term [T^{-1}].

Overland flow is included in the groundwater flux term of Eq. (1) (i.e. in the first term on the right hand side) using a free surface overland flow boundary condition that applies continuity of pressure and flux across the boundary between the land surface and the subsurface. Overland flow is solved using the kinematic wave approximation of the momentum equation where the diffusion terms are neglected and it is assumed that the bed slope, S_o [-] is equivalent to the friction slope. Flow varies as a function of ponded depth according to Manning's equation:

$$v = \frac{\sqrt{S_o}}{n} \psi_p{}^{2/3} \tag{2}$$

where n [$TL^{-1/3}$] is the Manning's roughness coefficient. Using this approach ParFlow is able to solve variably saturated groundwater flow and overland flow simultaneously. Practically this means that (1) the location of surface water bodies does not need to be specified a priori and will develop wherever water ponds in the domain, and (2) two-way groundwater surface water exchanges can evolve dynamically based on head gradients and subsurface properties.

ParFlow is also coupled with a land surface model derived from the Common Land Model (CLM) [*Dai et al.*, 2003]. In the combined ParFlow-CLM model [*Kollet and Maxwell*, 2008], ParFlow solves the water balance in the subsurface and CLM solves the combined water energy balance at the land surface. At the land surface, the energy balance (R_{net}) is comprised of sensible (H), latent (LE) and Ground (G) heat fluxes [Wm^{-2}]:

$$R_{net} = H + LE + G \tag{3}$$

All of the energy fluxes listed in Eq. (3) vary with soil moisture. CLM uses pressure head and saturation values for the upper subsurface layers (in this case the top 2m) simulated by ParFlow and passes infiltration fluxes back to ParFlow. Land surface processes are also driven by atmospheric forcing variables, which are provided as inputs to the model. Forcing variables include short and longwave radiation, precipitation, air temperature, atmospheric pressure, specific humidity and wind. Using these inputs, CLM simulates multiple land surface processes including canopy interception, evaporation from the canopy and the ground surface, plant transpiration, ground and sensible heat fluxes as well as snow dynamics.

This study focuses on simulated evapotranspiration E [LT^{-1}], which is the sum of evaporation, Ev and plant transpiration T. CLM uses a mass transfer approach with mean variables where evaporation is calculated using the gradient between the specific humidity at the ground surface, q_g [MM^{-1}], and the specific humidity at a reference

Hydrol. Earth Syst. Sci. Discuss., doi:10.5194/hess-2016-408, 2016
Manuscript under review for journal Hydrol. Earth Syst. Sci.
Published: 24 August 2016

Hydrology and Earth System Sciences
Discussions
Open Access
EGU

height, q_a [MM^{-1}], scaled by a soil resistance factor β [-], air density ρ_a and the atmospheric resistance, r_d [-] as follows:

$$Ev = -\beta \rho_a \frac{q_g - q_a}{r_d} \quad (4)$$

The soil resistance factor is calculated based on the saturation relative to the residual saturation and the saturation in the uppermost soil column (refer to *Jefferson and Maxwell* [2015] for the complete formulation).

Similarly transpiration is calculated by scaling the potential evapotranspiration to account for stomatal and aerodynamic resistance as follows

$$T = \left(R_{pp,dry} + L_w\right) L_{SAI} \left(\rho_a \frac{q_{sat} - q_a}{r_d}\right) \quad (5)$$

Here $R_{pp,dry}$ [-] is a scaling parameter, L_w [-]is the fraction of the canopy that is covered in water, L_{SAI} is leaf and stem area index and q_{sat} [-] is the saturated specific humidity [mm-1]. $R_{pp,dry}$ is a function of light and moisture limitations. Parameters that are used to determine leaf area index, reflectance and transmittance and root distributions vary by land cover type and are provided as inputs to the model using the 18 land cover classes defined by the International Geosphere Biosphere Program (IGBP). For additional details on the numerical approach and analysis on the sensitivity of evaporation and transpiration within CLM the reader is referred to [*Ferguson et al.*, 2016; *Jefferson and Maxwell*, 2015; *Kollet and Maxwell*, 2008; *Maxwell and Condon*, 2016].

2.3 Model domain and simulations

The analysis presented here is based on a previously developed transient ParFlow-CLM simulation of the majority of the Continental US (CONUS) documented in *Maxwell and Condon* [2016]. The CONUS domain covers the majority of eight major river basins, shown in Fig. 1 and spans roughly 6.3M square kilometers at 1km lateral resolution. As detailed in in *Maxwell and Condon* [2016] and *Maxwell et al.* [2015], the model extends 102 m below the subsurface with five vertical layers that contour to the land surface using a terrain following grid formulation [*Maxwell*, 2013]. The vertical resolution of the domain decreases with depth to better resolve the shallow subsurface. Layer thicknesses are 0.1, 0.3, 0.6, 1 and 100m moving from the land surface down. Spatially heterogeneous physical parameters for the subsurface include porosity, saturated hydraulic conductivity and van Genuchten parameters. Subsurface spatial units were determined using a national permeability map developed by *Gleeson et al.* [2011] for the bottom 100 m of the domain and the soil survey geographic database (SSURGO) for the top two meters. Maps of the subsurface units and their properties are available in *Maxwell and Condon* [2016] and *Maxwell et al.* [2015]. The land surface was derived from the Hydrologic data and maps based on the Shuttle Elevation Derivatives at multiple Scales (HydroSHEDS) digital elevation model using a topographic processing algorithm to ensure fully connected drainage network [*Barnes et al.*, 2016]. Vegetation types were extracted from the USGS land cover dataset using the IGBP land cover classifications.

The model was first initialized to a steady state groundwater configuration using the ParFlow model without CLM starting from a completely dry domain and providing a constant recharge forcing over the land surface to achieve a dynamic equilibrium. Development of this steady state simulation and evaluation of the resulting groundwater configuration are provided in [*Condon and Maxwell*, 2015; *Condon et al.*, 2015; *Maxwell et al.*, 2015]. Using the steady state groundwater configuration as a starting point, the coupled ParFlow-CLM model was used to simulate the fully transient system including land surface processes for water year 1985 (i.e. Oct. 1, 1984 through Sep., 30 1985), which was chosen as it is the most climatologically average within the past 30 years. The transient simulation was driven by historical hourly meteorological forcings from the North American Land Data Assimilation System Phase 2 (NLDAS 2) [*Cosgrove et al.*, 2003; *Mitchell et al.*, 2004]. Anthropogenic activities such as groundwater pumping and surface water storage are not included in the transient simulation. Therefore the simulation represents a pre-development interpretation of water year 1985, which is ideal for Budyko analysis. Complete details of the development of the transient simulation are available in *Maxwell and Condon* [2016].

The integrated physically based approach described above requires significant computational resources. The benefit of this computationally intensive approach is that it provides high-resolution (1 km^2) gridded outputs that fully define water and energy fluxes from the groundwater through the land surface without calibration and with a minimal number of empirical parameters. The transient simulation has been validated against publically available observations for the water year 1985 period. This includes transient observations at varying frequencies from 3,050 stream gauges, 29,385 groundwater wells and 378 snow stations for a total of roughly 1.2 million comparisons points. Flux tower observations were not available over this period, but latent heat fluxes were also compared to the Modern Era Retrospective-analysis for Research and Application (MERRA) dataset. Complete details of the model validation are provided in the supplemental information of *Maxwell and Condon* [2016]. Although there are of course limitations to the model, overall comparisons between simulated and observed values demonstrate that the modeling approach is robust; stream-flow timing and magnitude are generally well matched in undeveloped basins, snowpack timing and melt is accurate and spatial patterns in latent heat flux are reasonable.

2.4 Water Balance

Within ParFlow-CLM, incoming precipitation can infiltrate to the subsurface, contribute to runoff or pond. Evaporation occurs from ponded water, bare soil and canopy interception. Additionally, roots pull water from the subsurface to support transpiration for plants and lateral groundwater flow redistributes moisture within the subsurface and can further support overland flow. All of these processes occur within every 1 km^2 grid cell in the domain. The focus of this work is on watershed function and therefore the gridded results are aggregated to more hydrologically relevant units. The domain is divided into 33,454 subbasins each containing a single stream. Subbasin areas, outlined

Hydrol. Earth Syst. Sci. Discuss., doi:10.5194/hess-2016-408, 2016
Manuscript under review for journal Hydrol. Earth Syst. Sci.
Published: 24 August 2016

in Fig. 1, vary but are generally on the order of 100 km^2. The total drainage area for every subbasin, henceforth referred to as the watershed, is defined by tracing up the river network to encompass the entire upstream contributing area. This results in 33,454 nested watersheds ranging in drainage area from about one hundred square kilometers to over three million. For all of the following analysis we will focus on the 24,235 watersheds that are contained within the highlighted regions of Fig. 1. Similarly, while the simulation uses an hourly time step, here we evaluate annual values.

At the watershed scale, precipitation P [L^3] is balance by surface water outflows, Q_{out} [L^3], evapotranspiration, E [L^3], and groundwater surface water exchanges, referred to as groundwater contributions, G [L^3].

$$P = Q_{out} + E + G \quad (6)$$

Equivalently this can be expressed in terms of ratios relative to incoming precipitation where the sum of the outflow ratios sum to one:

$$1 = \frac{Q_{out}}{P} + \frac{E}{P} + \frac{G}{P} \quad (7)$$

As noted above, every watershed fully encompasses its contributing area, and therefore surface water inflows are zero. P is the sum of the gridded annual precipitation over the drainage area. Every watershed is defined to have a single outlet point. Q_{out} is the overland flow calculated hourly at the outlet using the ponded water depth and Eq. (2) and summed over the simulation period. E is the total evaporation and transpiration simulated by ParFlow-CLM summed fore every grid cell in the drainage area over the year. Groundwater contributions are calculated by using Eq. (6) as, P - Q_{out} - E. This approach results in a perfect water balance for every watershed. However, it is important to note that here G encompasses both exchanges between groundwater and surface water, which can be either positive fluxes from the surface to the subsurface or negative fluxes from subsurface to the surface, as well as changes in surface water storage. The assumption within this notation is that, over the annual simulation, changes in ponded water are small relative to groundwater surface water exchanges. Therefore we refer to the combined value as groundwater contributions and follow the convention that a positive groundwater contribution denotes water that is infiltrating from the land surface to the subsurface whereas a negative value indicates groundwater discharge which can either occur from groundwater supported E or baseflow contributions to streams.

In addition to the simulated evapotranspiration (E), potential evaporation E_p is calculated using Eq. (4), the hourly meteorological forcing data used to drive the simulations (air temperature, atmospheric pressure, specific humidity, and wind speed), and simulated ground temperatures in the uppermost layer of the model. To calculate potential evaporation, as opposed E, the β parameter is set to one to eliminate soil resistance and q_g is the saturated specific humidity calculated based on the ground temperature and atmospheric pressure. As with E, hourly gridded E_p values are summed over the entire simulation period for every watershed drainage area.

Fig. 2 maps the aridity index (E_p/P) as well as each component of the water balance from Eq. (7) expressed as ratios of precipitation. Subplots b and c show regional trends in the relative importance of evapotranspiration as opposed to overland flow. In the more arid western portions of the domain (shown in red on subplot a), Q_{out} is small compared to E whereas in the more humid eastern portions of the domain (blue and orange values in subplot a) the relative magnitude of Q_{out} increases. Within this annual simulation, subplot d shows that groundwater surface water exchanges can be a substantial portion of the water balance in much of the domain, indicating than an assumption of steady state is not valid for this simulation. The importance of groundwater contributions over this time frame is not surprising because the steady state assumption is generally applied over much longer time periods. The purpose of this work, however, is not to evaluate the conditions under which a steady state assumption will be valid or to predict changes in storage. Rather, we are taking advantage of the ability to directly calculate groundwater surface water exchanges

Hydrol. Earth Syst. Sci. Discuss., doi:10.5194/hess-2016-408, 2016
Manuscript under review for journal Hydrol. Earth Syst. Sci.
Published: 24 August 2016

within the simulation to evaluate the impact of these exchanges across a range of spatial scales and climates.

The groundwater contribution ratio map also illustrates the importance of lateral groundwater flow at multiple spatial scales within the system. Groundwater storage gains (i.e. positive values of *G/P*) are prevalent in the western arid portion of the domain and groundwater discharge to surface water is more common in the humid eastern portion of the domain. Within large basins like the Missouri, positive groundwater contributions occur in the headwater regions and transitions to negative values downstream. This is an illustration of lateral groundwater convergence and regional flow systems. Note that results are mapped by subbasin, but all water balance calculations are carried out for the complete watershed draining to a subbasin outlet. Therefore, Fig. 2 should be viewed as a system of nested subbasins with values representing progressively larger drainage areas as you move downstream. With this in mind, it is also intuitive that some of the largest groundwater contribution ratios occur in headwater basins while in downstream reaches on major rivers the values are smaller indicating a regional balance between local groundwater surface water exchanges.

2.5 Budyko analysis

We evaluate watershed behavior within the Budyko framework across a wide range of scales using the fully defined water balance components from the simulation, and the aridity index values calculated above. Budykyo's original formulation expressed evapotranspiration ratio as a function of aridity index (E_p/P) as follows [*Budyko*, 1974]:

$$\frac{E}{P} = \left\{\frac{E_p}{P}\left[1 - \exp\left(-\frac{E_p}{P}\right)\tanh\left(\frac{P}{E_p}\right)\ \right]\right\}^{0.5} \qquad (8)$$

Although the original analysis by Budyko did show some scatter around the curve, Eq. (8) defines a universal relationship that does not include any free parameters to account for spatial differences [*Budyko*, 1974]. Subsequent work has observed systematic variability between watersheds that can be related to climate, land cover and soil

Hydrol. Earth Syst. Sci. Discuss., doi:10.5194/hess-2016-408, 2016
Manuscript under review for journal Hydrol. Earth Syst. Sci.
Published: 24 August 2016

properties [e.g. *R. J. Donohue et al.*, 2007]. To reflect this, the original universal Budyko formulation has ben refined multiple times to include additional free parameters [*Choudhury*, 1999; *Fu*, 1981; *Milly*, 1994; *L. Zhang et al.*, 2001; *L. Zhang et al.*, 2004]. For a summary of these formulations refer to *Du et al.* [2016] and *L. Zhang et al.* [2004] .

Here we apply the commonly used Budyko formulation from *Fu* [1981] and *L. Zhang et al.* [2004]:

$$\frac{E}{P} = 1 + \frac{E_p}{P} - \left(1 + \left(\frac{E_p}{P}\right)^{\omega}\right)^{1/\omega} \qquad (9)$$

Eq. (9) includes one free parameter, ω which can range from one to infinity, henceforth referred to as the shape parameter. ω is an empirical parameter that has not been ascribed a specific physical meaning, but is generally conceptualized as an integrated catchment property that reflects characteristics such as land cover, soil properties, topography and seasonality [*L. Zhang et al.*, 2004]. Fig. 3 plots Eq. (8) for a range of ω values. The bold line (ω=2.6) is roughly equivalent to the original Budyko equation (Eq. 8) [*L. Zhang et al.*, 2004]. Following the original Budyko assumption of no change in storage, in humid locations where potential evaporation is less than precipitation, the system is energy limited and the maximum value of E is E_p. Conversely, when the aridity index is greater than one evapotranspiration the system is water limited and the maximum E/P value is one (indicating that all incoming precipitation is evaporated). As the shape parameter increases the curves moves progressively closer to the water (E/P=1) and energy (E/P=E_p/P) limitations of the system.

3. Results and discussion

3.1 Assessing the impacts of groundwater contributions using multiple water balance approaches

Fig. 3 follows the standard Budyko assumption that any incoming precipitation that does not contribute to evapotranspiration will leave the watershed as overland flow (i.e. E/P + Q_{out}/P =1). This is equivalent to assuming no change in storage, or zero groundwater contribution in Eq. (7). However, this may not always be the case for many reasons. For example, in the simulation evaluated here, the groundwater contribution fractions (*G/P*) mapped in Fig. 2d illustrate that groundwater is an important contributor to the water balance in many parts of the domain over the one year simulation period; often the groundwater contribution is greater than 10% of precipitation especially in small headwater basins. In this section we evaluate the impact of assuming that a basin is in equilibrium when groundwater contribution ratios are not zero using three different approaches to estimate the evapotranspiration ratio.

Precipitation and runoff are generally much easier to measure at the watershed scale than evapotranspiration or groundwater storage changes. Therefore, in many Budyko analyses evapotranspiration is not actually measured directly, but is calculated as the difference between precipitation and surface outflow [e.g. *Greve et al.*, 2015; *Istanbulluoglu et al.*, 2012; *Jones et al.*, 2012; *Renner et al.*, 2014; *T Wang et al.*, 2009; *Xu et al.*, 2013; *Yang et al.*, 2009]. This approach relies on the assumption that changes in storage are negligible. We refer to this as the *inferred evapotranspiration* approach and mimic it by approximating the evapotranspiration ratio as simulated $(P- Q_{out})/P$. The inferred approach is compared to the less common *direct evapotranspiration* approach where Budyko relationships are evaluated using observed evapotranspiration (or in this case the evapotranspiration that is simulated by our integrated hydrologic model). For the direct evapotranspiration approach Budyko relationships are evaluated using simulated *E/P*.

An alternate method that takes groundwater into account directly is to replace precipitation with effective precipitation, defined as precipitation minus groundwater contribution (*P-G*). This is the approach that was used by *Du et al.* [2016] in their study of Budyko relationships in arid basins. It should be noted here that the first two approaches (i.e. inferred and direct evapotranspiration) are commonly used in analyses that use the standard equilibrium assumption while the final method is designed for situations where this is not the case. By comparing results between all three, we consider the impact of nonzero groundwater contributions both for approaches that assume it is negligible, and for when it is accounted for.

Fig. 4 plots every watershed in the domain shown in Fig. 1 using the three approaches. All figures follow the Budyko curves, demonstrating that Budkyo relationships are recreated with the integrated hydrologic model. However, there are some notable differences between methods. For example, with the inferred *E* approach shown in subplot a, the points are focused near the water limit line (i.e. $(P- Q_{out})/P=1$) for high aridity values. Conversely, with the direct approach (subplot b), the evapotranspiration ratios are generally lower at high aridity values. Also, with the direct approach, there are points with evapotranspiration ratios are greater than one and fall above the water limit. This would appear to violate the water balance and will be discussed more later. When groundwater contributions are adjusted for using the effective precipitation approach show in subplot c, the points collapse more closely onto the Budyko curves.

Variability between approaches can be explained by the differences in the way groundwater contributions influence each method. This is illustrated in Fig. 5. In cases where G is zero, Fig. 5 demonstrates that the three formulations are equivalent. This is not the case when groundwater contributions are nonzero. When evapotranspiration is inferred from P-Q_{out} [as in:*Greve et al.*, 2015; *Istanbulluoglu et al.*, 2012; *Jones et al.*, 2012; *Renner et al.*, 2014; *T Wang et al.*, 2009; *Xu et al.*, 2013; *Yang et al.*, 2009], Eq. (7) shows that the result is actually *E+G* (and not *E*) so instead of evaluating,

$$\frac{E}{P} = f\left(\frac{E_p}{P}\right) \tag{10}$$

as intended in the Budyko formulation, this approach actually results in

$$\left(\frac{E}{P} + \frac{G}{P}\right) = f\left(\frac{E_p}{P}\right) \tag{11}$$

The direct approach avoids the limitations of the inferred approach by evaluating the evapotranspiration as intended in Eq. (10). However, groundwater storage changes will still influence the resulting behavior because the partitioning shown in Fig. 5b is now between evaporation and runoff plus groundwater contributions, not just runoff. This means that the maximum evapotranspiration fraction (i.e. the upper water limit) is not one, but one minus the groundwater contribution fraction. This shift in the limit explains the values greater than one in Fig. 4b; in these watersheds groundwater contributions are negative (i.e. groundwater supplying water to the land surface) and this allows for evapotranspiration values that are greater than the incoming precipitation. Similar shifts in the upper limits of the system for arid locations were found by *Potter and Zhang* [2009] who noted that evapotranspiration was actually approaching a fixed portion of potential evapotranspiration for high rainfall years in arid basins in Australia. Finally, in the effective precipitation case, the intent is to maintain focus on partitioning between evapotranspiration and overland flow so groundwater contributions are removed from the denominator of both ratios. This ensures that the modified outflow and evapotranspiration ratios will sum to one even when groundwater surface water exchanges are occurring.

For all three approaches we calculate the shape parameter for every point in the domain using Eq. (9). For the direct evapotranspiration approach we use Eq. (9) directly. For the inferred evapotranspiration approach we substitute in $(P\text{-}Q_{out})/P$ for E/P. For the effective precipitation approach we substitute in $E/(P\text{-}G)$ for E/P and $Ep/(P\text{-}G)$ for Ep/P. Fig. 6 a-c plot the resulting shape parameters as a function of groundwater contribution fraction colored by aridity. Both the inferred (6a) and direct approaches (6b) show clear, but contradictory, relationships with groundwater surface water exchanges. There is a positive relationship between the shape parameter and groundwater contribution fraction for the inferred evapotranspiration approach at the lower limits of the system as delineated by the dashed line in Fig. 6a. Because the groundwater contribution is included in the evapotranspiration fraction when evapotranspiration is inferred from precipitation and runoff (i.e. $P\text{-}Q_{out} = E + G$), nonzero groundwater contributions will contribute directly to the evapotranspiration fraction as shown in Fig. 5a. If a constant positive groundwater contribution is applied across aridity values this would result in a vertical shift the Budyko curve relative to a zero groundwater contribution system as illustrated in Fig. 6d. Moving vertically within the Budyko plot results in higher shape parameters (as shown in Fig. 3). Therefore, the vertical shifting shown in Fig. 6d will result in a positive correlation between groundwater contribution fraction and shape parameter.

When the direct evapotranspiration approach is applied (6b), groundwater contributions are now lumped in with the outflow fraction (Fig. 5b). In this case, positive groundwater contributions can be conceptualized as shifting the limits of what is available for evapotranspiration. This is illustrated by the shifting limit lines in Fig. 6e where the upper water limitation on the system shifts from 1 to 1-G/P and the energy limitation shifts from E_p/P to E_p/P-G/P. This creates a nonlinear inverse relationship between curve number and groundwater contributions. As the groundwater contribution fraction increases, the decreasing upper bounds on evapotranspiration fraction will bias the system towards lower curve numbers (refer to Fig. 3). This is a nonlinear relationship which can be shown by calculating the shape parameter as a function of groundwater contribution fraction in Eq. (9) for the limiting case where there is no outflow (i.e. G/P=1-E/P). The dashed line on Fig. 6b shows the resulting relationship for a relatively high aridity value of 6. The curve provides a good approximation for the upper limit of Fig. 5b.

The effective precipitation case shows the least correlation with groundwater contribution fraction. This is to be expected because the purpose of this approach is to adjust for groundwater contributions before calculating shape parameters. However, it should be noted that some dependence on groundwater contribution is still to be expected the extent that groundwater surface water exchanges are also correlated with other watershed properties. This is true for the other approaches too. While the effect of groundwater contributions within each space can be precisely determined using Eq. (7) and Eq. (9), it is important to note that the watersheds evaluated here are also heterogeneous in land cover, topography and seasonality. Therefore, in the scatter plots shown in Fig. 6, the relationships between shape parameters and groundwater contribution explained by subplots d and e appear as limits rather than strong predictors. This point is also made by *Istanbulluoglu et al.* [2012] who used the inferred evapotranspiration approach. They provide a similar conceptual model to Fig. 6d for the shifting effect of storage changes on behavior. However, for the four basins in Nebraska that they evaluated they found a negative relationship between inferred evapotranspiration ratios and aridity that was attributed to a strong negative correlation between groundwater contribution fraction and aridity index.

Fig. 7 compares the shape parameters calculated with each approach to illustrate the way that different assumptions can bias derived Budyko relationships. Subplot a shows the differences between the inferred and direct evapotranspiration approaches, which are commonly used in studies that assume no change in storage. Because groundwater contributions are incorporated into different components of the water balance with these methods Fig. 7a shows that, for positive groundwater contributions (green points), the inferred shape parameters are systematically higher than the direct shape parameters, while the inverse is true when groundwater contributions are negative (purple points). Furthermore, when groundwater contributions are large (i.e. the dark green circles in subplot a), the direct method has uniformly low shape parameters, but the inferred method still shows a range of shape parameters. This is to be expected from Figs. 6 b and e that show that for high groundwater contributions the upper limit of the evapotranspiration ratio is limited by surface water 'losses' to groundwater and as a result all of the points will be pushed to low curve numbers.

The direct and inferred evapotranspiration methods are also compared to the effective precipitation approach, which does account for groundwater contributions (Fig.7 b &c). As would be expected, the direct and inferred methods have inverse biases; shape parameters are systematically higher with the inferred approach relative effective precipitation and lower for the direct approach. Here too the trends with groundwater contributions are reversed with positive contributions creating a positive bias for the inferred case and a negative bias for the effective precipitation case. Also, there is a much stronger correlation between curve numbers between the inferred evapotranspiration and effective precipitation approaches than with the direct evapotranspiration approaches. This is partially due to the loss of curve number sensitivity for high groundwater contribution fractions with the direct approach which is also shown in subplot a. For all three cases, Fig. 7 demonstrates systematic variability in the shape parameter even for relatively small groundwater contributions.

3.2 Spatial patterns and scaling

The influence of catchment characteristics such as vegetative properties, topography and climate on Budyko relationships has been well established by previous studies[e.g. *Li et al.*, 2013; *Milly*, 1994; *Shao et al.*, 2012; *Williams et al.*, 2012; *Xu et al.*, 2013; *Yang et al.*, 2009; *Yokoo et al.*, 2008]. As such, spatial variability in shape parameters is to be expected even after adjusting for groundwater contributions. Fig. 8 maps shape parameters for the nested watersheds calculated using three different approaches. All three maps demonstrate local variability and regional trends in the shape parameters.

Spatial patterns are consistent between approaches in the more humid eastern portion of the domain, where groundwater contribution ratios are generally smaller (Fig. 2d), but in the more arid western portion of the domain significant differences are observed. For both the inferred evapotranspiration and effective precipitation approaches there are large red areas indicating curve numbers greater than four where the evapotranspiration ratio is falling very close to the water limitation. The areas with curve numbers greater than four are generally consistent between the inferred evapotranspiration and effective precipitation approaches, but the inferred precipitation approach results in higher curve numbers throughout the western portion of the domain than the effective precipitation approach. This is consistent with the biases shown in Fig. 5b. Conversely, with the direct evapotranspiration approach the western portion of the domain has much lower shape parameters and less spatial

Hydrol. Earth Syst. Sci. Discuss., doi:10.5194/hess-2016-408, 2016
Manuscript under review for journal Hydrol. Earth Syst. Sci.
Published: 24 August 2016

variability. Again, this finding is consistent with Fig. 6b and e, which show that when groundwater contributions are high, the curve numbers are uniformly low because the flux from the surface water system to the groundwater shifts the upper limit of the evapotranspiration fraction down. The systematic differences in Fig. 8, both with respect to the shape parameter values and the spatial patterns, where groundwater surface water exchanges are occurring indicate the potential to arrive at fundamentally different conclusions depending on what approach is used.

Xu et al. [2013] built a neural network model to predict shape parameters using long-term observations from 224 watersheds with drainage areas ranging from 100 to 10,000 km^2. They then predicted shape parameters globally using a variety of catchment characteristics. Excluding the small drainage areas with shape parameters greater than four, the spatial patterns calculated here with the effective precipitation approach match well with the global map presented by *Xu et al.* [2013]. Even though the one-year transient simulation used for the analysis presented does not meet the equilibrium criteria, Figs. 4c and 8c show that realistic Budyko relationships are still found when groundwater contributions are accounted for using the effective precipitation approach.

Furthermore, for our system we can compare results by drainage area. Budyko originally limited analysis to large basins (which he defined as drainage areas greater than 10,000 km^2) where he argued that macroclimate can be expected to dominate partitioning [*Budyko*, 1974]. Indeed subsequent work has shown that for smaller areas vegetation dynamics becoming increasingly important [*R. J. Donohue et al.*, 2007]. Fig. 9 plots Budyko relationships for every watershed grouped by drainage area using the effective precipitation formulation as an example. In this figure, the drainage area is increased from watersheds less than 100 km^2 (9a) to watersheds greater than 100,000 km^2 (9d). This figure shows that the scatter decreases as drainage area increases and the points converge around a single curve. This behavior illustrates increased importance of local watershed characteristics for smaller drainage areas consistent with previous studies.

This is further demonstrated by Fig. 10, which shows the interquartile range of shape parameters for each approach with increasing drainage area. In all three cases, we observe a decrease in variance moving from small to large basins and a trend of decreasing shape parameters with increasing area. Again this indicates increased importance of watershed characteristics at smaller scales. In the case of the inferred and direct evapotranspiration approaches, because groundwater contributions are not accounted for in the calculations, some of this variability can also be attributed to spatial patterns in groundwater surface water exchanges and lateral groundwater flow. The inferred evapotranspiration and effective precipitation approaches are the most similar while the direct evapotranspiration formulation is systematically lower and less variable (this is also consistent with the maps shown in Fig. 9). For the largest drainage areas, the median shape parameter is 1.8 for the inferred evapotranspiration approach, 1.5 for the direct evapotranspiration approach and 1.7 using effective precipitation.

The shape parameters estimated with the effective precipitation approach are arguably the most relevant to other long-term studies that have assumed equilibrium conditions. Our simulated median value is slightly lower than the original Budyko value of 2.6 and the median value of 2.56 found by [*Greve et al.*, 2015] using the 411 Model Parameter Estimation Experiment (MOPEX) catchments in the US. However, it compares well with 1.8 median value for large MOPEX basins in the US reported by *Xu et al.* [2013]. Although, it should be noted that *Xu et al.* [2013] report a higher 2.6 median value for small basins, and the median small basin value reported found here is 2.0. Part of this bias can likely be attributed to the concentration of MOPEX basins in the eastern portion of the US where Fig. 9 shows that shape parameters are generally higher. Overall, the consistency in spatial patterns and convergence around the Budkyo curve for large drainage areas indicates that the ParFlow-CLM model recreates Budyko relationships even over a relatively short annual time. However, for smaller watersheds variability in catchment characteristics is still an important consideration.

4. Summary and Conclusions

Hydrol. Earth Syst. Sci. Discuss., doi:10.5194/hess-2016-408, 2016
Manuscript under review for journal Hydrol. Earth Syst. Sci.
Published: 24 August 2016

Hydrology and Earth System Sciences Discussions
Open Access

For this study, we use a one-year integrated groundwater surface water simulation of the majority of the continental US to evaluate Budyko relationships. We focus on the implications of assuming equilibrium in systems where we can demonstrate that systematic groundwater surface water exchanges are occurring over many spatial scales. Using the integrated modeling approach allows us to directly calculate every component of the water balance. Taking advantage of this we recreate multiple approaches used in Budyko analysis: (1) inferring evapotranspiration from precipitation and runoff assuming no storage changes, (2) using the evapotranspiration directly simulated by the model but not accounting for groundwater contributions in the Budyko formulation and (3) accounting for groundwater contributions using a modified approach where the total available water is calculated by subtracting groundwater contributions from precipitation to determine 'effective precipitation'.

Results show that with both the inferred and direct evapotranspiration approaches even small groundwater contribution fractions can influence the result. Over large watersheds, the two evapotranspiration methods converged to different shape parameters, 1.8 for inferred evapotranspiration and 1.5 for direct evapotranspiration. We also demonstrate that the same groundwater contribution ratio will alter Budkyo curve differently depending on whether evapotranspiration is evaluated directly or inferred. With the inferred evapotranspiration approach, groundwater contributions are inherently included in the evapotranspiration ratio, so it shifts points vertically on the Budyko plot; whereas when evapotranspiration is used directly, groundwater contributions essentially shift the limits of what is available to be partitioned into overland flow or evapotranspiration.

This fundamental difference means that comparisons between basins can be significantly altered depending on what approach is used if groundwater surface water exchanges are occurring. We show that for both methods the shape parameter varies as a function of groundwater contribution ratio, especially in arid watersheds. As a result, the two approaches produce different spatial patterns in shape parameters. In both cases it is simple to demonstrate how a constant groundwater contribution value will

Hydrol. Earth Syst. Sci. Discuss., doi:10.5194/hess-2016-408, 2016
Manuscript under review for journal Hydrol. Earth Syst. Sci.
Published: 24 August 2016

shift the Budyko curve for all aridity values. However, because groundwater surface water exchanges are spatially heterogeneous and depend on aridity as well as other watershed characteristics, the impact of variable groundwater contributions across a large sample of watersheds is difficult to predict. For example, some recent studies that have evaluated the impact of groundwater storage changes in a small number of arid basins have shown that the correlation between recharge to groundwater and aridity leads to an inverse relationship between evapotranspiration fraction and aridity [*Istanbulluoglu et al.*, 2012; *T Wang et al.*, 2009]. For larger studies that include a more diverse set of watersheds correlations between groundwater contribution ratios may not be as clear; still, our results indicate that groundwater contributions are an important consideration when evaluating scatter between watersheds within the Budyko framework.

Using the effective precipitation approach demonstrated by *Du et al.* [2016] we are able to directly account for groundwater contributions within the Budyko framework. Results with this formulation demonstrate that consistent Budkyo relationships can be developed even when groundwater surface water exhanges violate the steady state assumption, as long as they can be quantified and appropriately adjusted for. After accounting for groundwater contributions, there is still significant variability in the shape parameters between small watersheds, which is to be expected given the other heterogeneities in watershed characteristics across the domain. We find that for larger basins, the points converge around a single curve. Interestingly, the two methods that do not account for groundwater contributions also converge around a single curve for large watersheds although they result in different shape parameters.

One of the primary assumptions of the Buydko hypothesis is that watersheds are in equilibrium and there are no changes in storage. This means that all incoming precipitation will either leave the watershed as evapotranspiration or overland flow. While the Budyko curve has been well verified with observations from around the globe, it is now widely accepted that the relationship between evapotranspiration ratios and aridity indices is not universal and that some additional curve parameters are need to

Hydrol. Earth Syst. Sci. Discuss., doi:10.5194/hess-2016-408, 2016
Manuscript under review for journal Hydrol. Earth Syst. Sci.
Published: 24 August 2016

account for spatial variability between watersheds. Many subsequent studies have related curve parameters from various Budyko formulations to catchment properties such as vegetation, topography and seasonality. However, very few studies evaluate the validity of the equilibrium assumption over their study period. Furthermore, because long-term evapotranspiration estimates at the watershed scale are seldom available many infer that evapotranspiration is the difference between precipitation and outflow.

Using an integrated model, we demonstrate that changes in groundwater storage and lateral flow can also contribute to variability between watersheds in systematic ways and that different approaches based on the equilibrium assumption will yield different results when this assumption is not met. While these results indicate the potentially significant implications of ignoring groundwater contributions within Budyko analyses, it should be noted that both groundwater surface water exchanges and evapotranspiration are difficult to measure over large scales and long-term records similar to stream gauges are often not available. We acknowledge that the common approach of developing a water balance using precipitation and streamflow alone is generally necessitated by data availability not ignorance. For this study, we take advantage of a sophisticated hydrologic simulation that allows us to define every flux in the domain and balance water perfectly, but this is not the case for most observational studies. Furthermore, even within this fully defined approach, we acknowledge that even the most sophisticated numerical model is a gross simplification of the natural system. Therefore, the intention of these comparisons is not to discredit previous approaches, rather to illustrate the potential impacts of incorrectly assuming equilibrium conditions across a broad range of physiographic settings and spatial scales. Our results show that even when changes in storage are occurring, large watersheds still roughly follow Budyko curve; however the shape parameter and scatter will vary with groundwater contribution and depending on how evapotranspiration is quantified. This indicates that, even if groundwater contributions are not included directly into analyses, it is vital provide some quantification of uncertainty in water balance closure in order to

Hydrol. Earth Syst. Sci. Discuss., doi:10.5194/hess-2016-408, 2016
Manuscript under review for journal Hydrol. Earth Syst. Sci.
Published: 24 August 2016

determine whether differences in shape parameters are actually resulting from unique basin characteristics or uncertainty in storage.

Data Availability:

All data from this analysis are available upon request. Instructions for accessing the ParFlow simulations used here are provided in [*Maxwell et al.*, 2016].

Acknowledgements:

Funding for this work was provided by the US Department of Energy Office of Science, Offices of Advanced Scientific Computing Research and Biological and Environmental Sciences IDEAS project. The ParFlow simulations were also made possible through high-performance computing support from Yellowstone (ark:/85065/d7wd3xhc) provided by National Center for Atmospheric Research's Computational and Information Systems Laboratory, sponsored by the National Science Foundation.

Works Cited

Barnes, M. L., C. Welty, and A. J. Miller (2016), Global Topographic Slope Enforcement to Ensure Connectivity and Drainage in an Urban Terrain, *Journal of Hydrologic Engineering*, *21*(4), 06015017. doi:10.1061/(ASCE)HE.1943-5584.0001306

Budyko, M. I. (1958), The Heat Balance of the Earth's Surface, U.S. Department of Commerce, Weather Bureau, Washington D.C.

Budyko, M. I. (1974), *Climate and LIfe*, Academic Press, New York.

Choudhury, B. (1999), Evaluation of an empirical equation for annual evaporation using field observations and results from a biophysical model, *Journal of Hydrology*, *216*(1–2), 99-110. http://dx.doi.org/10.1016/S0022-1694(98)00293-5

Condon, L. E., and R. M. Maxwell (2015), Evaluating the relationship between topography and groundwater using outputs from a continental-scale integrated hydrology model, *Water Resources Research*, n/a-n/a. 10.1002/2014WR016774

Condon, L. E., A. S. Hering, and R. M. Maxwell (2015), Quantitative assessment of groundwater controls across major US river basins using a multi-model regression algorithm, *Advances in Water Resources*, *82*, 106-123. http://dx.doi.org/10.1016/j.advwatres.2015.04.008

Cosgrove, B. A., D. Lohmann, K. E. Mitchell, P. R. Houser, E. F. Wood, J. C. Schaake, A. Robock, C. H. Marshall, J. Sheffield, Q. Duan, L. Luo, R. W. Higgins, R. T. Pinker, D. J. Tarpley, and J. Meng (2003), Real-time and retrospective forcing in the North American Land Data Assimilation System (NLDAS) project, *J. Geophys. Res.*, *108*(D22). 10.1029/2002JD003118

Dai, Y., X. Zeng, R. E. Dickinson, I. Baker, G. B. Bonan, M. G. Bosilovich, A. S. Denning, P. A. Dirmeyer, P. R. Houser, G. Niu, K. W. Oleson, C. A. Schlosser, and Z.-L. Yang (2003), The Common Land Model, *Bulletin of the American Meterorological Society*, *84*(8), 1013-1023. 10.1175/BAMS-84-8-1013

Donohue, R. J., M. L. Roderick, and T. R. McVicar (2007), On the importance of including vegetation dynamics in Budyko's hydrological model, *Hydrol. Earth Syst. Sci.*, *11*(2), 983-995. 10.5194/hess-11-983-2007

Donohue, R. J., M. L. Roderick, and T. R. McVicar (2011), Assessing the differences in sensitivities of runoff to changes in climatic conditions across a large basin, *Journal of Hydrology*, *406*(3–4), 234-244. http://dx.doi.org/10.1016/j.jhydrol.2011.07.003

Du, C., F. Sun, J. Yu, X. Liu, and Y. Chen (2016), New interpretation of the role of water balance in an extended Budyko hypothesis in arid regions, *Hydrol. Earth Syst. Sci.*, *20*(1), 393-409. 10.5194/hess-20-393-2016

Ferguson, I. M., J. L. Jefferson, R. M. Maxwell, and S. J. Kollet (2016), Effects of root water uptake formulation on simulated water and energy budgets at local and basin scales, *Environmental Earth Sciences*, *75*(4), 1-15. 10.1007/s12665-015-5041-z

Fu, B. P. (1981), On the calculation of the evaporation from land surface (in Chinese), *Sci. Atmos. Sin.*, *5*, 23-31.

Hydrol. Earth Syst. Sci. Discuss., doi:10.5194/hess-2016-408, 2016
Manuscript under review for journal Hydrol. Earth Syst. Sci.
Published: 24 August 2016

Hydrology and Earth System Sciences
Discussions
Open Access
EGU

Gentine, P., P. D'Odorico, B. R. Lintner, G. Sivandran, and G. Salvucci (2012), Interdependence of climate, soil, and vegetation as constrained by the Budyko curve, *Geophysical Research Letters*, *39*(19), n/a-n/a. 10.1029/2012GL053492

Gleeson, T., L. Smith, N. Moosdorf, J. Hartmann, H. H. Durr, A. H. Manning, L. P. H. van Beek, and A. M. Jellinek (2011), Mapping permeability over the surface of the Earth, *Geophysical Research Letters*, *38*(L02401). 10.1029/2010GL045565

Greve, P., L. Gudmundsson, B. Orlowsky, and S. I. Seneviratne (2015), Introducing a probabilistic Budyko framework, *Geophysical Research Letters*, *42*(7), 2261-2269. 10.1002/2015GL063449

Istanbulluoglu, E., T. Wang, O. M. Wright, and J. D. Lenters (2012), Interpretation of hydrologic trends from a water balance perspective: The role of groundwater storage in the Budyko hypothesis, *Water Resources Research*, *48*(3), n/a-n/a. 10.1029/2010WR010100

Jefferson, J. L., and R. M. Maxwell (2015), Evaluation of simple to complex parameterizations of bare ground evaporation, *Journal of Advances in Modeling Earth Systems*, *7*(3), 1075-1092. 10.1002/2014MS000398

Jones, J. A., I. F. Creed, K. L. Hatcher, R. J. Warren, M. B. Adams, M. H. Benson, E. Boose, W. A. Brown, J. L. Campbell, and A. Covich (2012), Ecosystem processes and human influences regulate streamflow response to climate change at long-term ecological research sites, *BioScience*, *62*(4), 390-404.

Kollet, S. J., and R. M. Maxwell (2006), Integrated surface ‐ groundwater flow modeling: A free ‐ surface overland flow boundary condition in a parallel groundwater flow model, *Advances in Water Resources*, *29*(7), 945-958. 10.1016/j.advwatres.2005.08.006

Kollet, S. J., and R. M. Maxwell (2008), Capturing the influence of groundwater dynamics on land surface processes using an integrated, distributed watershed model, *Water Resources Research*, *44*(W02402). 10.1029/2007WR006004

Koster, R. D., and M. J. Suarez (1999), A Simple Framework for Examining the Interannual Variability of Land Surface Moisture Fluxes, *Journal of Climate*, *12*(7), 1911-1917. doi:10.1175/1520-0442(1999)012<1911:ASFFET>2.0.CO;2

Li, D., M. Pan, Z. Cong, L. Zhang, and E. Wood (2013), Vegetation control on water and energy balance within the Budyko framework, *Water Resources Research*, *49*(2), 969-976. 10.1002/wrcr.20107

Maxwell, R. M. (2013), A terrain-following grid transform for parallel, large-scale, integrated hydrologic modeling, *Advances in Water Resources*, *53*, 109-117. 10.1016/j.advwatres.2012.10.001

Maxwell, R. M., and N. L. Miller (2005), Development of a coupled land surface and groundwater model, *Joural of Hydrometerology*, *6*(3), 233-247. doi:10.1175/JHM422.1

Maxwell, R. M., and L. E. Condon (2016), Connections between groundwater flow and transpiration partitioning, *Science*, *353*(6297), 377-380. DOI: 10.1126/science.aaf7891

Maxwell, R. M., L. E. Condon, and S. J. Kollet (2015), A high resolution simulation of groundwater and surface water over most of the continental US with the

Hydrol. Earth Syst. Sci. Discuss., doi:10.5194/hess-2016-408, 2016
Manuscript under review for journal Hydrol. Earth Syst. Sci.
Published: 24 August 2016

integrated hydrologic model ParFlow v3, *Geoscientific Model Development*, *8*, 923-937. 10.5194/gmd-8-1-2015

Maxwell, R. M., L. E. Condon, S. J. Kollet, K. Maher, R. Haggerty, and M. M. Forrester (2016), The imprint of climate and geology on the residence times of groundwater, *Geophysical Research Letters*, *43*(2), 701-708. 10.1002/2015GL066916

Milly, P. C. D. (1994), Climate, soil water storage, and the average annual water balance, *Water Resources Research*, *30*(7), 2143-2156. 10.1029/94WR00586

Milly, P. C. D., and K. A. Dunne (2002), Macroscale water fluxes 2. Water and energy supply control of their interannual variability, *Water Resources Research*, *38*(10), 24-21-24-29. 10.1029/2001WR000760

Mitchell, K. E., D. Lohmann, P. R. Houser, E. F. Wood, J. C. Schaake, A. Robock, B. A. Cosgrove, J. Sheffield, Q. Duan, L. Luo, R. W. Higgins, R. T. Pinker, D. J. Tarpley, D. P. Lettenmaier, C. H. Marshall, J. K. Entin, M. Pan, W. Shi, V. Koren, J. Meng, B. H. Ramsay, and A. A. Bailey (2004), The multi-institution North American Land Data Assimilation System (NLDAS): Utilizing multiple GCIP products and partners in a continental distributed hydrological modeling system, *J. Geophys. Res.*, *109*(D07S90). 10.1029/2003JD003823

Potter, N. J., and L. Zhang (2009), Interannual variability of catchment water balance in Australia, *Journal of Hydrology*, *369*(1–2), 120-129. http://dx.doi.org/10.1016/j.jhydrol.2009.02.005

Renner, M., K. Brust, K. Schwärzel, M. Volk, and C. Bernhofer (2014), Separating the effects of changes in land cover and climate: a hydro-meteorological analysis of the past 60 yr in Saxony, Germany, *Hydrol. Earth Syst. Sci.*, *18*(1), 389-405. 10.5194/hess-18-389-2014

Shao, Q., A. Traylen, and L. Zhang (2012), Nonparametric method for estimating the effects of climatic and catchment characteristics on mean annual evapotranspiration, *Water Resources Research*, *48*(3), n/a-n/a. 10.1029/2010WR009610

Troch, P. A., G. Carrillo, M. Sivapalan, T. Wagener, and K. Sawicz (2013), Climate-vegetation-soil interactions and long-term hydrologic partitioning: signatures of catchment co-evolution, *Hydrol. Earth Syst. Sci.*, *17*(6), 2209-2217. 10.5194/hess-17-2209-2013

Van Genuchten, M. T. (1980), A Closed-form Equation for Predicting the Hydraulic Conductivity of Unsaturated Soils, *Soil Science Society of America*, *44*(5), 892-898.

Wang, D. (2012), Evaluating interannual water storage changes at watersheds in Illinois based on long-term soil moisture and groundwater level data, *Water Resources Research*, *48*(3), n/a-n/a. 10.1029/2011WR010759

Wang, T., E. Istanbulluoglu, J. Lenters, and D. Scott (2009), On the role of groundwater and soil texture in the regional water balance: An investigation of the Nebraska Sand Hills, USA, *Water Resources Research*, *45*(10), n/a-n/a. 10.1029/2009WR007733

Hydrol. Earth Syst. Sci. Discuss., doi:10.5194/hess-2016-408, 2016
Manuscript under review for journal Hydrol. Earth Syst. Sci.
Published: 24 August 2016

Hydrology and Earth System Sciences
Open Access
Discussions

Williams, C. A., M. Reichstein, N. Buchmann, D. Baldocchi, C. Beer, C. Schwalm, G. Wohlfahrt, N. Hasler, C. Bernhofer, T. Foken, D. Papale, S. Schymanski, and K. Schaefer (2012), Climate and vegetation controls on the surface water balance: Synthesis of evapotranspiration measured across a global network of flux towers, *Water Resources Research*, *48*(6), n/a-n/a. 10.1029/2011WR011586

Xu, X., W. Liu, B. R. Scanlon, L. Zhang, and M. Pan (2013), Local and global factors controlling water-energy balances within the Budyko framework, *Geophysical Research Letters*, *40*(23), 6123-6129. 10.1002/2013GL058324

Yang, D., F. Sun, Z. Liu, Z. Cong, G. Ni, and Z. Lei (2007), Analyzing spatial and temporal variability of annual water-energy balance in nonhumid regions of China using the Budyko hypothesis, *Water Resources Research*, *43*(4), n/a-n/a. 10.1029/2006WR005224

Yang, D., W. Shao, P. J. F. Yeh, H. Yang, S. Kanae, and T. Oki (2009), Impact of vegetation coverage on regional water balance in the nonhumid regions of China, *Water Resources Research*, *45*(7), n/a-n/a. 10.1029/2008WR006948

Yokoo, Y., M. Sivapalan, and T. Oki (2008), Investigating the roles of climate seasonality and landscape characteristics on mean annual and monthly water balances, *Journal of Hydrology*, *357*(3–4), 255-269. http://dx.doi.org/10.1016/j.jhydrol.2008.05.010

Zhang, L., W. R. Dawes, and G. R. Walker (2001), Response of mean annual evapotranspiration to vegetation changes at catchment scale, *Water Resources Research*, *37*(3), 701-708. 10.1029/2000WR900325

Zhang, L., N. Potter, K. Hickel, Y. Zhang, and Q. Shao (2008), Water balance modeling over variable time scales based on the Budyko framework – Model development and testing, *Journal of Hydrology*, *360*(1–4), 117-131. http://dx.doi.org/10.1016/j.jhydrol.2008.07.021

Zhang, L., K. Hickel, W. R. Dawes, F. H. S. Chiew, A. W. Western, and P. R. Briggs (2004), A rational function approach for estimating mean annual evapotranspiration, *Water Resources Research*, *40*(2), n/a-n/a. 10.1029/2003WR002710

Hydrol. Earth Syst. Sci. Discuss., doi:10.5194/hess-2016-408, 2016
Manuscript under review for journal Hydrol. Earth Syst. Sci.
Published: 24 August 2016

Hydrology and Earth System Sciences
Open Access
Discussions

Figures:

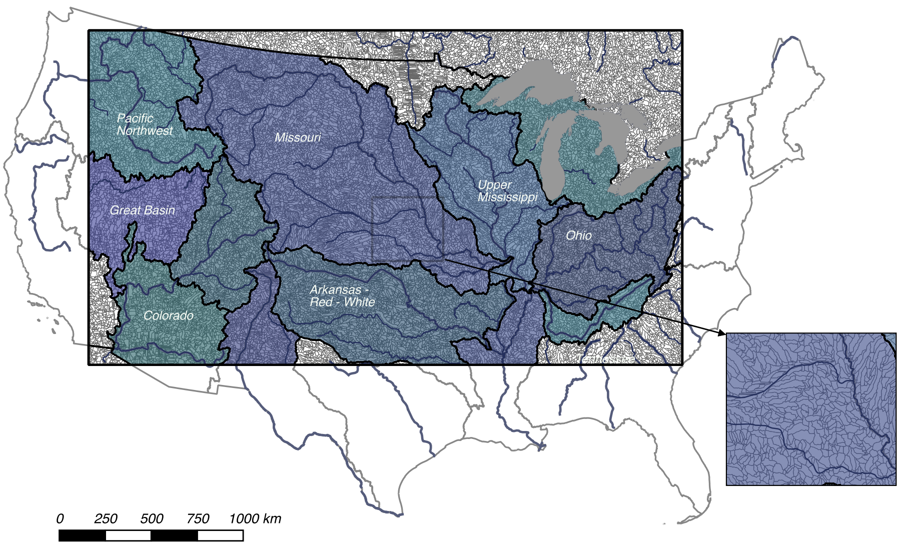

Figure 1: Map of the simulation domain extent (black box) with major river basins highlighted and labeled. Subbasins within the domain are outlined in grey. Major rivers are show in blue for reference (Note that the simulated river network is much more highly resolved as illustrated in [Maxwell et al., 2015])

Hydrology and Earth System Sciences
Discussions
Open Access

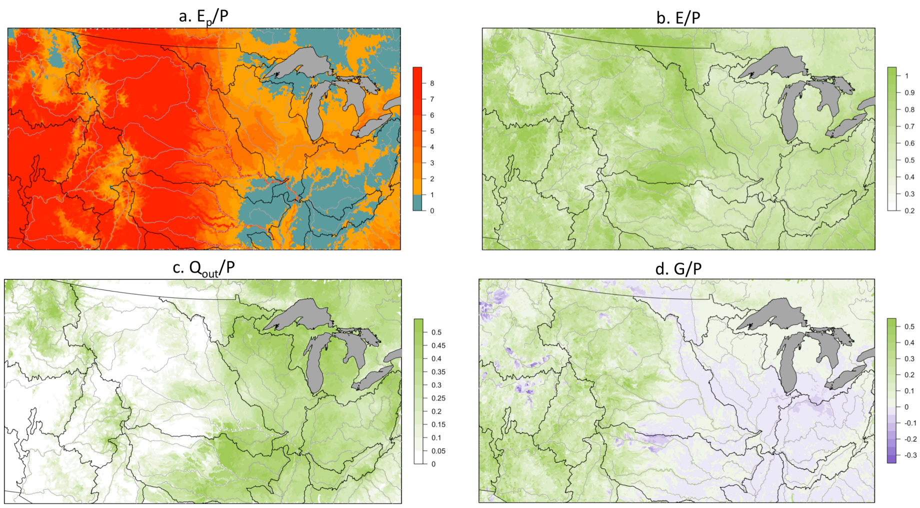

Figure 2: Maps of (a) aridity index (Ep/P) and the ratios of (b) evapotranspiration (c) outflow and (d) groundwater contributions compared to precipitation. Major river basins are outlined in black. Note that ratios are mapped according to the subbasins shown in Fig. 1 but the values reflect the water balance for the entire watershed. This is a system of nested watersheds so the value for each watershed is reported at its outlet subbasin.

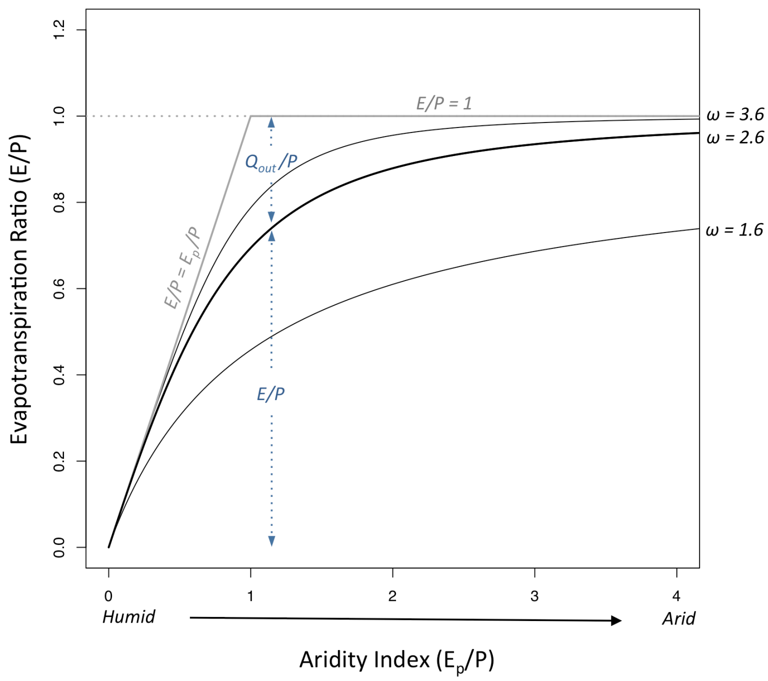

Figure 3: Illustration of the Budkyo framework showing curves with three different shape parameters (black lines, ω=1.6, 2.6 and 3.6) in relation to the water (E/P=1) and energy (E/P=E_p/P) limits of the system, grey lines.

Hydrol. Earth Syst. Sci. Discuss., doi:10.5194/hess-2016-408, 2016
Manuscript under review for journal Hydrol. Earth Syst. Sci.
Published: 24 August 2016

Hydrology and Earth System Sciences
Open Access
Discussions

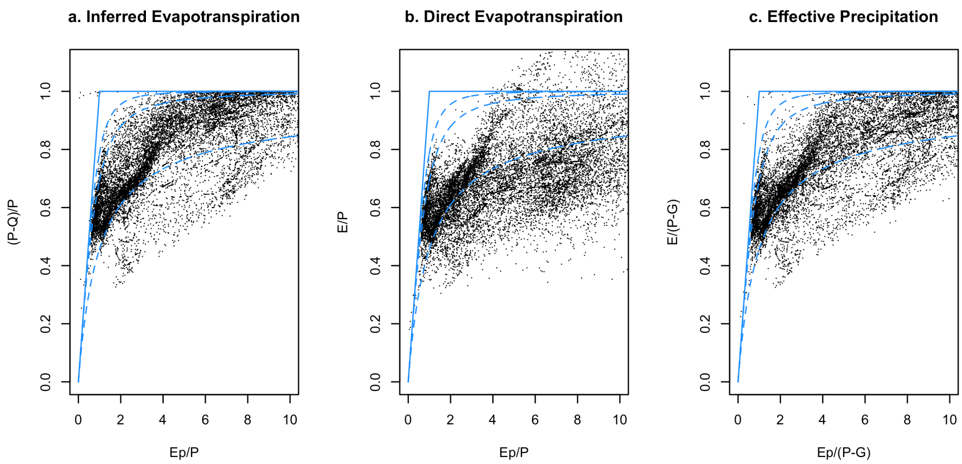

Figure 4: Budyko plots for the three approaches (a) inferred evapotranspiration, (b) direct evapotranspiration and (c) effective precipitation with points for every watershed in the domain. Dashed blue lines are Budkyko curves with ω values of 1.6, 2.6 and 3.6 and the solid blue lines are the water and energy limits (refer to Fig. 3).

Hydrol. Earth Syst. Sci. Discuss., doi:10.5194/hess-2016-408, 2016
Manuscript under review for journal Hydrol. Earth Syst. Sci.
Published: 24 August 2016

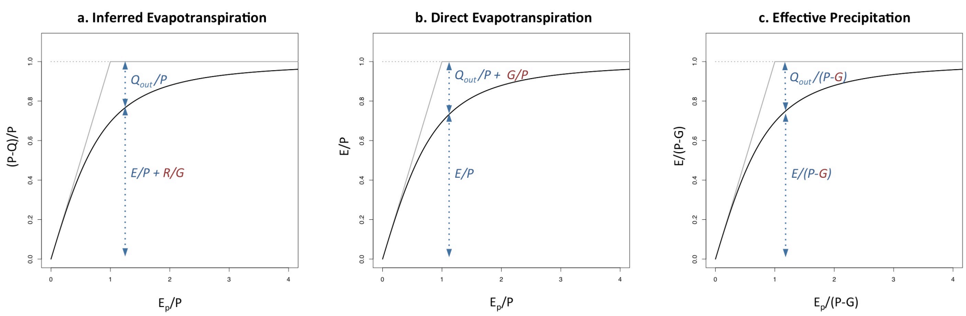

Figure 5: Illustration of the treatment of groundwater contributions for each of the three approaches. The black lines show the water and energy limits and an example Budyko curve, similar to Fig. 3. Arrows indicate the water balance component represented above and below the curve in each case.

Hydrol. Earth Syst. Sci. Discuss., doi:10.5194/hess-2016-408, 2016
Manuscript under review for journal Hydrol. Earth Syst. Sci.
Published: 24 August 2016

Hydrology and Earth System Sciences
Discussions
Open Access

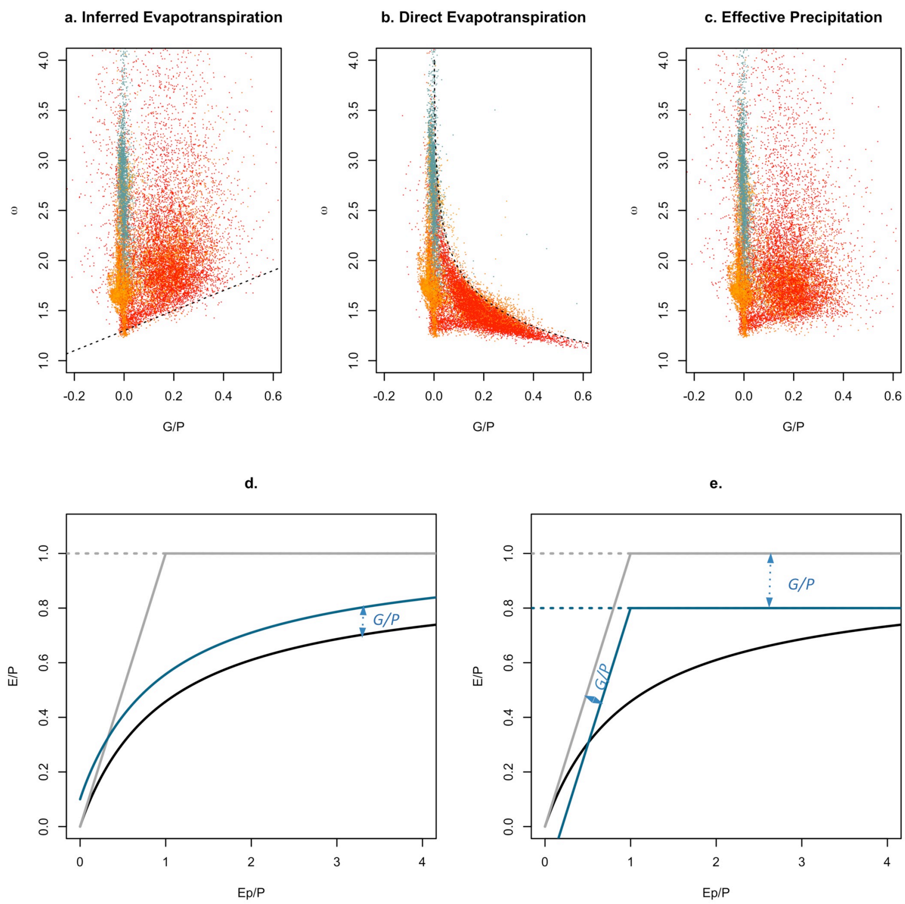

Figure 6: Comparison of shape parameters to groundwater contribution ratios for the three approaches in every watershed (a-c). Points are colored by aridity as shown in Fig. 2a. A dashed line with a slope of one is included on (a) for reference. The dashed line on (b) shows the relationship between the shape parameter and groundwater contribution fraction for an example aridity value of six in the limiting case where outflow is zero. The conceptual figures below illustrate the impact of a positive groundwater contribution (i.e. a net flux from the surface to the subsurface) for (d) the inferred evapotranspiration and (e) direct evapotranspiration approaches.

Hydrol. Earth Syst. Sci. Discuss., doi:10.5194/hess-2016-408, 2016
Manuscript under review for journal Hydrol. Earth Syst. Sci.
Published: 24 August 2016

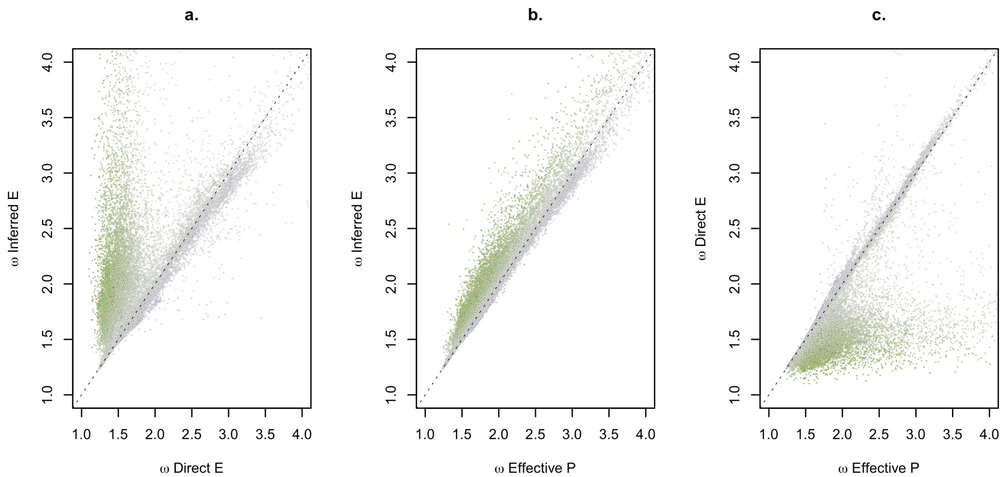

Figure 7: Comparison of shape parameters between the three approaches for every watershed. Points are colored by groundwater contribution fraction as shown in Fig. 2d. The dashed line on each plot is a one to one line for reference.

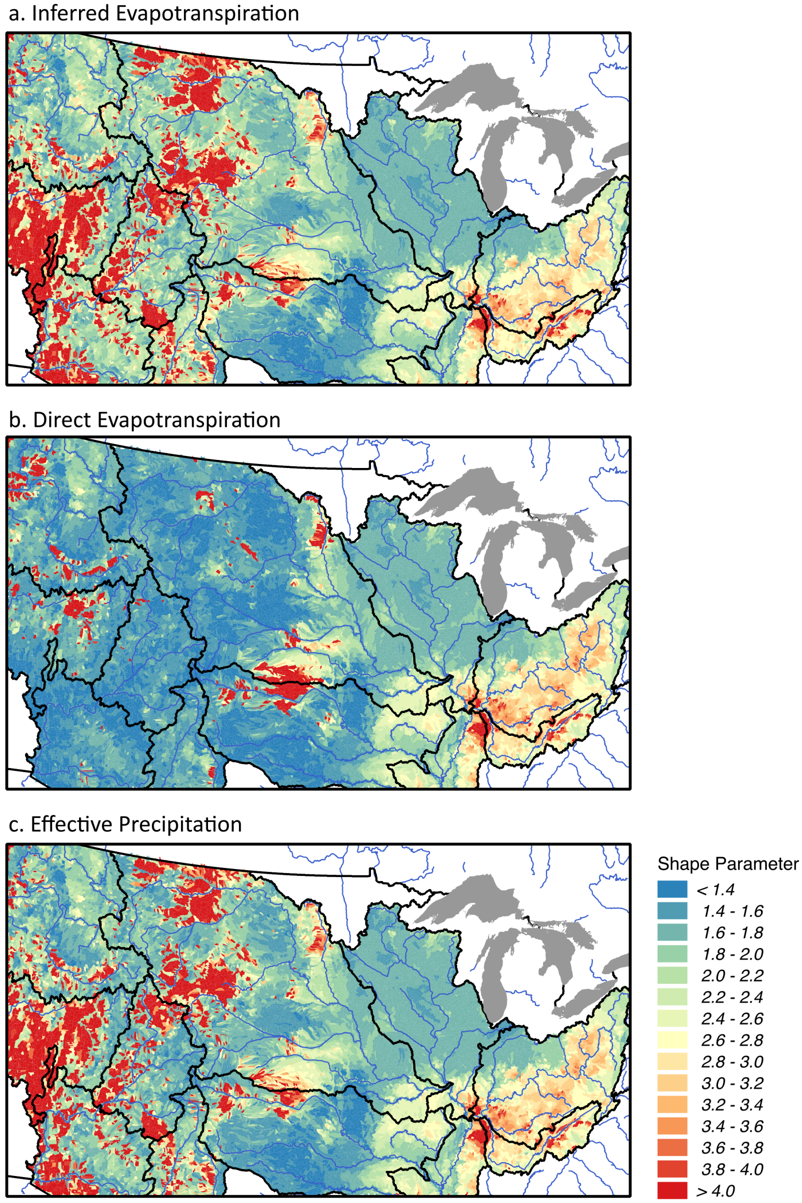

Figure 8: Map of shape parameters calculated for the 24,235 nested watersheds using the (a) inferred evapotranspiration, (b) direct evapotranspiration and (c) effective precipitation. Major rivers are outlined in blue and regional boundaries in black.

Hydrol. Earth Syst. Sci. Discuss., doi:10.5194/hess-2016-408, 2016
Manuscript under review for journal Hydrol. Earth Syst. Sci.
Published: 24 August 2016

Hydrology and Earth System Sciences Discussions
Open Access

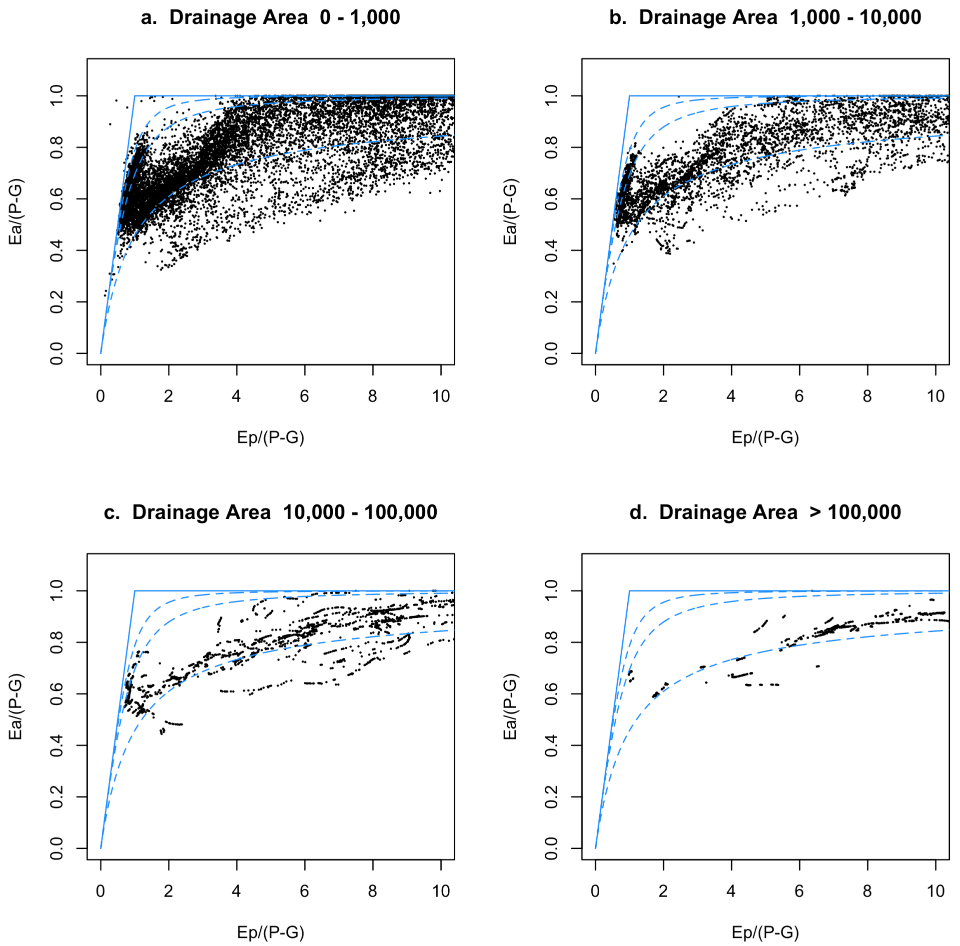

Figure 9: Budyko plots of evapotranspiration ratio versus aridity index using the effective precipitation method with watersheds grouped by drainage area [km^2]. Blue dashed lines are Budkyo curves with shape parameters of 1.6, 2.6 and 3.6 (refer to Fig. 3) and the solid blue lines show the water and energy limits.

Hydrol. Earth Syst. Sci. Discuss., doi:10.5194/hess-2016-408, 2016
Manuscript under review for journal Hydrol. Earth Syst. Sci.
Published: 24 August 2016

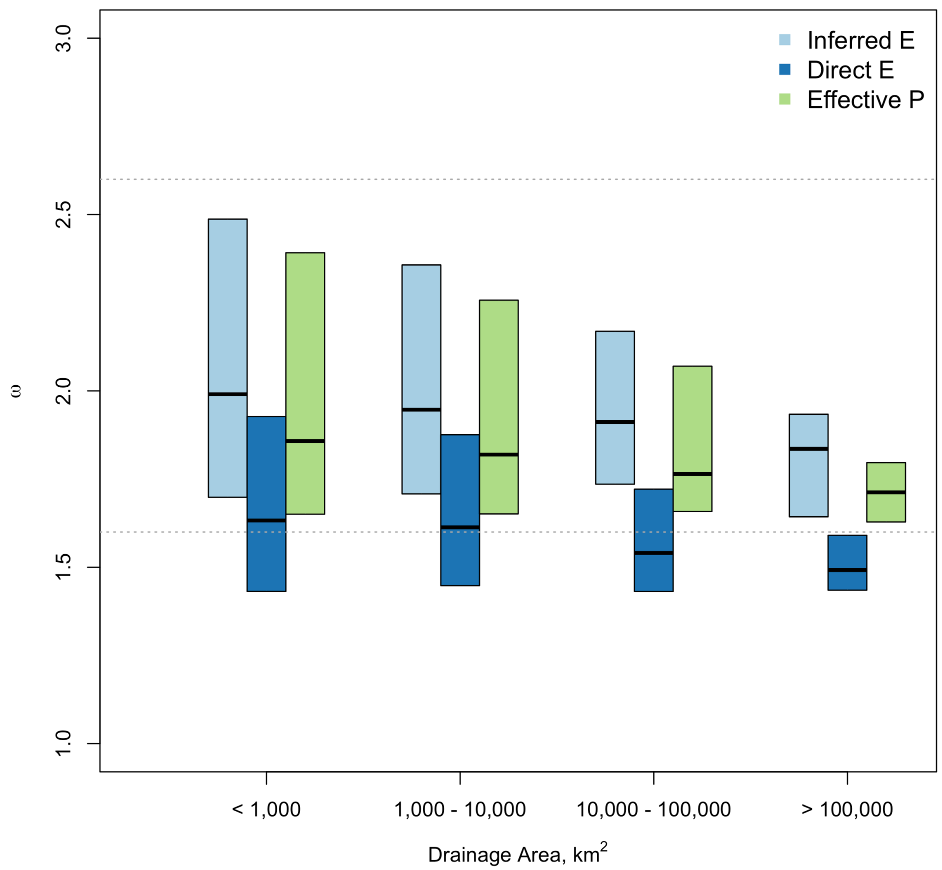

Figure 10: Boxplots showing the interquartile range (i.e. 25-75th percentile values) of shape parameters for all three approaches grouped by drainage area. Dashed lines are at 1.6 and 2.6 for reference.